Comparison of the liquid-ordered bilayer phases containing cholesterol or 7-dehydrocholesterol in modeling Smith-Lemli-Opitz syndrome[S]

Galya Staneva,[1],* Claude Chachaty,[†] Claude Wolf,[†] and Peter J. Quinn[§]

Institute of Biophysics,* Bulgarian Academy of Sciences, Sofia, Bulgaria; Laboratoire commun de spectrométrie,[†] Université Pierre et Marie Curie, Paris, France; and Biochemistry Department,[§] King's College London, London, UK

Abstract The phase behavior of egg sphingomyelin (ESM) mixtures with cholesterol or 7-dehydrocholesterol (7-DHC) has been investigated by independent methods: fluorescence microscopy, X-ray diffraction, and electron spin resonance spectroscopy. In giant vesicles, cholesterol-enriched domains appeared as large and clearly delineated domains assigned to a liquid-ordered (L_o) phase. The domains containing 7-DHC were smaller and had more diffuse boundaries. Separation of a gel phase assigned by X-ray examination to pure sphingomyelin domains coexisting with sterol-enriched domains was observed at temperatures less than 38°C in binary mixtures containing 10-mol% sterol. At higher sterol concentrations, the coexistence of liquid-ordered and liquid-disordered phases was evidenced in the temperature range 20°–50°C. Calculated electron density profiles indicated the location of 7-DHC was more loosely defined than cholesterol, which is localized precisely at a particular depth along the bilayer normal. ESR spectra of spin-labeled fatty acid partitioned in the liquid-ordered component showed a similar, high degree of order for both sterols in the center of the bilayer, but it was higher in the coexisting disordered phase for 7-DHC. The differences detected in the models of the lipid membrane matrix are said to initiate the deleterious consequences of the Smith-Lemli-Opitz syndrome.—Staneva, G., C. Chachaty, C. Wolf, and P. J. Quinn. **Comparison of the liquid-ordered bilayer phases containing cholesterol or 7-dehydrocholesterol in modeling the Smith-Lemli-Opitz syndrome.** *J. Lipid Res.* **2010.** 51: 1810–1822.

Supplementary key words membrane rafts • SLO • sphingomyelin

A malformation syndrome bearing the name of the authors was described by Smith, Lemli, and Opitz in 1964 (1).

The cause was subsequently shown to be related to blockade of the ultimate reaction in the biosynthesis of cholesterol (2). Recessive mutations were described of the gene coding for 7-dehydrocholesterol reductase, the enzyme responsible for catalyzing the final reduction of 7-dehydrocholesterol to cholesterol. A variety of deleterious mutations for 7-dehydrocholesterol reductase with distinct geographic distribution have been shown (3) and traced with a noticeably high frequency around 1% in healthy heterozygote carriers (4).

The accumulation in fetal tissue of the metabolite 7-dehydrocholesterol (7-DHC) and derivative isomer 8-dehydrocholesterol is a specific biomarker for antenatal diagnosis of this severe condition (5) involving the central nervous system (6), masculinization, and facial and limb defects (7, 8). Indeed the accumulation of precursors is constantly associated with a severe deficit of the end-product cholesterol, which is also judged deleterious for embryo development. The teratology was originally studied by this laboratory in animal models treated with potent inhibitors of cholesterol biosynthesis (9). The results of in vivo studies are considered inconclusive with respect to whether the cholesterol deficit or the accretion of aberrant sterol competing with membrane cholesterol is the underlying mechanism for teratology. The administration of a diet highly enriched in cholesterol to inhibitor-treated pregnant dams was proven to suppress malformations in the offspring (10). Nevertheless, it cannot be concluded that the deficit in cholesterol alone is causal because negative

Abbreviations: Chol, cholesterol; 7-DHC, 7-dehydrocholesterol; EPC, egg yolk L-α-phosphatidylcholine; ESM, egg yolk sphingomyelin; ESR, electron spin resonance; GUV, giant unilamellar vesicle; L_d, liquid disordered; L_o, liquid ordered; SAXS, small-angle X-ray scattering; SLO, Smith-Lemli-Opitz syndrome; WAXS, wide-angle X-ray scattering; XRD, X-ray diffraction.

[1] To whom correspondence should be addressed.
e-mail: gstaneva@obzor.bio21.bas.bg
[S] The online version of this article (available at http://www.jlr.org) contains supplementary data in the form of three figures.

feedback on the aberrant sterol production is also exerted by cholesterol supplied in excess (11, 12).

There are currently two hypotheses to explain the cell defects of Smith-Lemli-Opitz syndrome (SLO) embryonic cells. The first is that 7-DHC is not able to substitute for cholesterol as a component of cell membranes and, second, that the cleavage of the morphogenic protein, Sonic Hedgehog (SHH) is defective in the presence of 7-DHC. Both cholesterol and 7-DHC are known to augment cleavage of the N-terminal signaling peptide from SHH (13). Because the reaction to remove the signal peptide takes place in membrane "raft" domains that are enriched in cholesterol, the two explanations for SLO syndrome may be reconciled. It is possible that replacement of cholesterol by 7-DHC produces membrane domains that are unable to provide the necessary structural environment for posttranslational modification of SHH (14).

There is some evidence that 7-DHC produces defective membrane rafts. Studies of the replacement of cholesterol with 7-DHC in preparations of hippocampal membranes in vitro failed to restore the binding activity of the serotonin 1A receptor despite the overall recovery of the membrane lipid order (15, 16). Although the total sterol (7-DHC *plus* cholesterol) incorporation in rafts isolated from AY9944-treated rat brains reaches levels similar to that of cholesterol incorporation in control preparations, the raft protein profiles are different (17), suggesting that the sterol composition changes the lipid arrangement that, in turn, influences protein sorting and defective signaling functions (14). Another difference has been reported in mast cells derived from Dhcr7$^{-/-}$ mice accumulating 7-DHC in lipid rafts in vivo (18). 7-DHC was assumed to disrupt the raft stability in Dhcr7$^{-/-}$ mice and, consequently, to produce a dysfunctional allergic response because of a loosening of the raft association of the regulatory *Lyn* kinase. Furthermore, the molecular simulation has shown that 7-DHC is found less effective compared with cholesterol in condensing the packing density of acyl chains (19). In model membrane studies, 7-DHC is known to partition into domains that were resistant to the solubilization by Triton X-100 and more stable at higher temperatures than cholesterol (20).

To understand the molecular mechanisms that underlie these observations, biophysical studies that can distinguish the subtle differences in membrane structure and stability when 7-DHC substitutes for cholesterol are required. The presence of only an additional double bond in the B-ring of the sterol nucleus contrasts with the profound consequences in embryos when the precursor replaces the end-metabolite. Cholesterol is an absolute requirement for a number of homeothermic animal species. K. Bloch postulated that sterol structure is gradually optimized during evolution by adding steps to the biosynthetic pathway to perform new functions (21). A concerted coevolution of sphingolipids and sterols in mammals is also postulated along with this sterol-only hypothesis.

The present study of model membrane systems was undertaken using three methods with complementary spatial and time scales to compare the properties of sterols. Fluorescence probe partition has been used to characterize domain separation on the micrometer scale in giant unilamellar vesicles (GUV) comprised of ternary mixtures of sphingomyelin and sterol within a fluid phospholipid matrix. Synchrotron X-ray diffraction (XRD) studies of binary mixtures of sphingomyelins and sterols have been performed at the molecular scale to investigate the association of major raft components over a temperature range spanning the gel-to-fluid phase transition of the sphingomyelin. Finally, the dynamic properties of phases formed by sphingomyelin and sterol have been examined at a molecular and nanosecond scale using electron spin resonance (ESR) of spin-labeled probes to determine the differences between sterols in maintenance of molecular ordering. We demonstrate that subtle differences in the simple membrane models can be detected between cholesterol and its precursor 7-dehydrocholesterol. We conclude that the observed differences may explain the molecular basis of defective raft assembly in embryonic cells that results in Smith-Lemli-Opitz syndrome.

MATERIALS AND METHODS

Lipids

Lipids were used without further purification: egg yolk L-α-phosphatidylcholine (EPC), egg yolk sphingomyelin (ESM), cholesterol (CHOL), and 7-dehydrocholesterol (7-DHC) were obtained from Sigma (Sigma-Aldrich Chimie SARL, St. Quentin, France). The fluorescent phospholipid analog Texas Red [1, 2-dihexadecanoyl-*sn*-glycero-3-phosphoethanolamine, triethylammonium salt (TR-DHPE)] was purchased from Invitrogen (Eugene, OR). The molar ratios of lipids in ternary mixtures of EPC/ESM/sterol, (45/45/10, 40/40/20, 34/33/33) were chosen for GUV studies for comparison with the lipid composition of detergent-resistant membrane fractions. For example, SM/CHOL ratios reported in detergent-resistant membrane preparations vary widely from 1/1 to 2/1 (22). Inclusion of a fluid lipid (EPC) is a technical requirement to observe partition of a fluorescent probe between liquid-disordered (L$_d$) phase and liquid-ordered (L$_o$) phase in GUVs. For ESR and XRD studies, comparisons between the two sterols in binary mixtures was the more appropriate system to distinguish subtle differences in the association of the major components of membrane rafts in forming a liquid-ordered structure.

Preparation of giant unilamellar vesicles

The electroformation method developed by Angelova and Dimitrov (23) was used to form the vesicles. Binary and ternary mixtures of EPC, ESM, and sterol were prepared, in which all lipid ratios are given as molar. GUVs were formed in a temperature-controlled chamber. We followed the particular protocol for unilamellar giant heterogeneous vesicles formation described elsewhere (24). Electroformation temperature was chosen to be the maximal temperature at which a high yield of vesicles was consistently obtained. Although deposited lipids are uniformly mixed, each vesicle varied slightly in composition (25). This composition error is estimated to be ∼2%, which could be observed as different miscibility transition temperatures and brightness (mol% dye) between vesicles. The head-group–labeled lipid analog TR-DHPE is excluded from the more ordered phase for its steric hindrance and partitions predominantly in the disordered phase, which makes the ordered phase appear as a dark area within the bright fluid vesicle membrane.

GUVs comprised of binary mixtures of SM/sterols exhibited homogeneous appearance on the micron scale. Obviously, the gel/liquid-ordered phase separation that takes place on the submicron scale is not detectable at the actual resolution.

Video microscopy

The vesicles were observed using a Zeiss Axiovert 135 microscope, equipped with a 63× long working distance objective lens (LD Achroplan Ph2). The observations were recorded using a Zeiss AxioCam HSm CCD camera connected to an image recording and processing system (Axiovision, Carl Zeiss, Wien, Austria). The phase morphology transformations of the heterogeneous GUV membrane were followed in fluorescence by the Zeiss filter set Ex/Em = 546/590 nm. As a function of time, fusion and alteration of the domain shape and size can be spotted by video microscopy.

Synchrotron X-ray diffraction methods

Samples for XRD examination were prepared by dissolving lipids in warm (45°C) chloroform/methanol (2:1, v/v) and mixing in the desired proportions (given as molar ratio). The organic solvent was subsequently evaporated in SpeedVac equipment (SPD111V, Savant, Thermo Fisher, Illkirch, France). The dry lipids were hydrated with an equal weight of water and heated repeatedly above 45°C, a temperature cycling which was found efficient to fully hydrate a control of pure SM (26, 27). Simultaneous small- and wide-angle X-ray scattering intensities were recorded during thermal scans between 20° and 50°C on beamline 2.1 of the Daresbury SRS as described elsewhere (27).

Analysis of X-ray diffraction data

The SAXS intensity profiles were analyzed using fitting by Gaussian/Lorentzian symmetrical functions. The scattering intensity data from the first five orders of the Bragg reflections from the multilamellar liposomes were used to construct electron density profiles (28). After correcting the raw data by subtracting the background scattering from both water and the sample cell, each of the Bragg peaks were fitted by a Gaussian/Lorentzian (Voigt) distribution using PeakFit 4.12 (Systat Software). The protocol has been recently described in (27, 29).

ESR spectroscopic methods

The ESR experiments have been performed at 9.4 GHz using the doxyl-16-stearic spin probe denoted hereafter as 16NS. In the whole temperature range of the experiments (12°–47°C), the reorientation of this probe is under the fast motional regime with correlation times $\tau \ll 2$ ns (**Table 1**). The experimental procedures and methods of determining ESR parameters from spectral fittings have been reported elsewhere (30, 31).

In the present study and for most of the samples, the spectral fittings have been performed under the following assumptions: (1) One anisotropic (liquid crystalline) site; (2) two sites (anisotropic and isotropic); (3) two anisotropic sites. The most- and the less-ordered sites are denoted A and B, respectively.

The selection among these assumptions is based on the quality of the fits estimated from the standard deviation between the experimental and fitted spectra, normalized with respect to the maximum amplitude of the former, as well as the identification of the phases detected by X-ray diffraction. (See supplementary Fig. III for an example of the fit obtained with the spectral simulation method.) The parameters of major interest are the order parameter S_{zz} of the Z-axis of the nitrogen hyperfine coupling tensor parallel to the C_{15}—C_{17} vector of the stearoyl chain and the fraction of A/B sites. As the partition coefficients of 16NS into the various phases are unknown, the fractions of sites do not

TABLE 1. Parameters of spin-label motion in binary mixtures of egg yolk sphingomyelin (ESM) with different proportions of cholesterol or 7-DHC: Reorientation correlation times

Samples	Activation Energies	$\tau_{37°}$
	kJ/mol	*ns*
SM 83%, CHOL 17%	20.2	0.83
SM 66%, CHOL 34%	26.6	0.38
SM 59%, CHOL 41%	24.5	0.33
SM 50%, CHOL 50%	22.3	0.34
SM 40%, CHOL 60%	28.4	0.30
SM 83%, 7DHC 17%	20.3	1.00
SM 66%, 7DHC 34%	24.1	0.41
SM 59%, 7DHC 41%	23.4	0.30
SM 50%, 7DHC 50%	21.3	0.35
SM 40%, 7DHC 60%	20.6	0.40

Parameters are from the least-squares fittings of the following equation:

$$\tau = \tau_{37°} \exp\left[\frac{E}{R}\left(\frac{1}{T} - \frac{1}{310} \right) \right]$$

Abbreviations: Chol, cholesterol; 7-DHC, 7-dehydrocholesterol; ESM, egg sphingomyelin.

represent the fractions of coexisting phases but likely have similar temperature dependence.

RESULTS

Phase behavior in GUVs

Domain separation of ordered and disordered phases in phospholipid/sterol mixtures was examined by fluorescence microscopy of GUVs. Vesicles composed of EPC/ESM/sterol in molar proportions 45/45/10 were examined at different temperatures in **Fig. 1**. At temperatures from 42°C down to 22°C, a GUV containing one or the other sterol has exhibited a homogeneous appearance on the microscopic scale [Fig. 1A(a), B(a)]. Reduction of the temperature to 20°C results in the emergence of domains in the micrometer range. Dark domains correspond to areas where the fluorescent probe is excluded. Dark, round-shaped domains were observed in mixtures with cholesterol [Fig. 1A(b)]. Domain size is increased by subsequent fusion events as the temperature is reduced [Fig. 1A(c–e)]. Domain fusion typically occurs in less than 1 s, and the round shape of the dark domain is quickly restored after fusion. The separation of dark domains is reminiscent of liquid/liquid immiscibility between the liquid-ordered (dark area) domains and the liquid-disordered (bright area) domains previously described (32–34).

Domain patterns in GUV containing 7-DHC were different (Fig. 1B). Two types of dark domains were distinguished at 15°–20°C with crenellated borders or leaf-like domains [Fig. 1B(b, c)]. Unlike cholesterol, in the presence of 7-DHC, the dark domains do not fuse but tend to cluster and form a "necklace" of small-size domains [Fig. 1B(c)]. Note that dark domains assigned as liquid-ordered domains do not fuse together as do domains assigned to the liquid-ordered phase in the presence of cholesterol [Fig. 1B(d, e)]. The properties of the 7-DHC domains appear similar to gel domains observed in the absence of
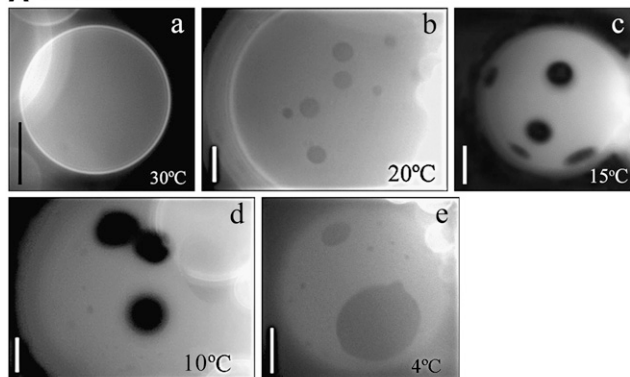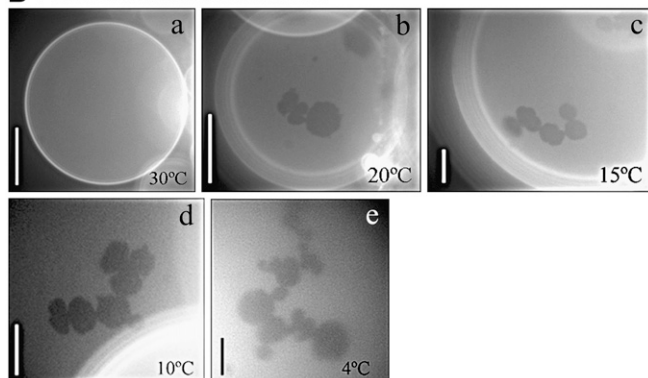
Fig. 1. Domain morphology in ternary mixtures of EPC/ESM/ sterol (45/45/10 mol%). (A) cholesterol (B) 7-dehydrocholesterol. Domain separation was revealed using the fluorescent lipid Texas red-DPPE (1 mol%). Observation temperatures are reported as indicated. Bar = 20 µm. EPC, egg yolk L-α-phosphatidylcholine; ESM, egg yolk sphingomyelin.

sterol in control binary mixtures composed of equimolar proportions of EPC/ESM (see supplementary Fig. I). This observation suggests that the presence of 7-DHC up to 10 mol% is not sufficient to create detectable liquid-ordered domains. Moreover, the observation of GUVs composed of greater proportions of sterols [EPC/ESM/sterol, 40/40/ 20 (**Fig. 2**) and 34/33/33 (**Fig. 3**)] supports a consistent and clear-cut difference between cholesterol and 7-DHC to produce a separate phase.

The addition of cholesterol 20 mol% in ternary mixtures results in the enlargement of dark areas assigned to L_o phase [Fig. 2A(a)] compared with mixtures containing 10 mol% cholesterol. At 20°C [Fig. 2A(b)] multiple, small L_o domains emerge initially and fuse shortly after into few large domains [Fig. 2A(c–e)]. The domains have a round shape owing to the "minimized tension" line energy at the rim of the two fluid phases by optimizing the area/perimeter ratio. The mixtures containing 7-DHC show small dark domains that have an irregular round shape, and unlike cholesterol, they did not change significantly with temperature [Fig. 2B(b)]. Occasionally the clusters of two, three, or more quasiround small domains observed in the presence of 7-DHC remained connected by fine filaments [Fig. 2B(c–f)] and moved in concert in the membrane

plane. Notably, no "leaf-like" gel domains were detected in the presence of 20 mol% 7-DHC, even at temperatures of 4°C, indicating that the sterol was intermixed with sphingomyelin. The overall domain area in the presence of 20 mol% 7-DHC was roughly similar to the area of L_o domain formed in the presence of cholesterol, however, the rate of fusion of 7-DHC domains remained relatively slow. Moreover, domains demonstrated plasticity during fusion compared with the fast, elastic behavior observed in cholesterol mixtures.

The higher molar proportion of sterol in ternary mixtures (33 mol%) resulted in the formation of dark domains at a temperature 3°C lower [Fig. 3A, B(b)] than in the presence 20 mol%. Clusters of small-size domains were also decreased, and a single enlarged domain was occasionally observed at 33 mol% [Fig. 3B(c)]. The domain pattern was more regularly rounded compared with mixtures containing less 7-DHC. As the dark area was enlarged with fewer separated domains, the observation was consistent with fusion. Nevertheless, fusion in the presence of 7-DHC proceeds at a slow rate, and observations have rarely captured fusion events.
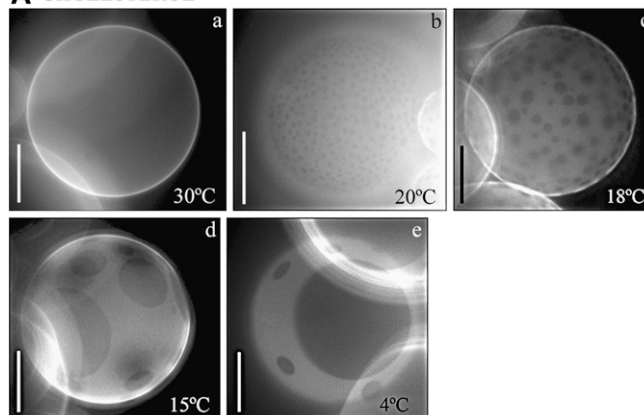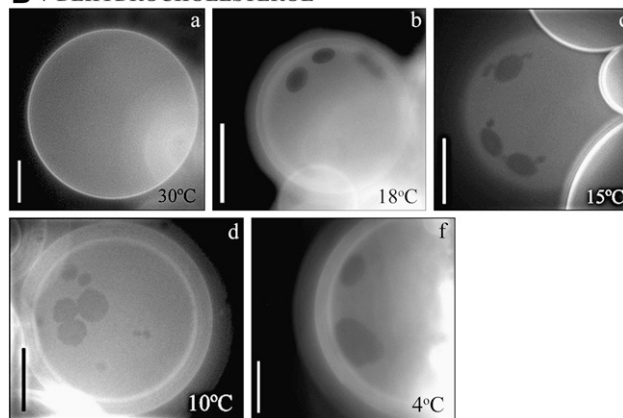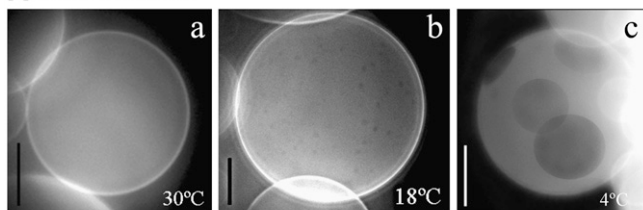

Fig. 2. Domain morphology in ternary mixtures of EPC/ESM/ sterol (40/40/20 mol%) as a function of temperature: (A) cholesterol and (B) 7-dehydrocholesterol probed by fluorescent lipid Texas red-DPPE (1 mol%). Bar 20 µm. EPC, egg yolk L-α-phosphatidylcholine; ESM, egg yolk sphingomyelin.

Liquid-ordered phases in SLO syndrome **1813**

A CHOLESTEROL

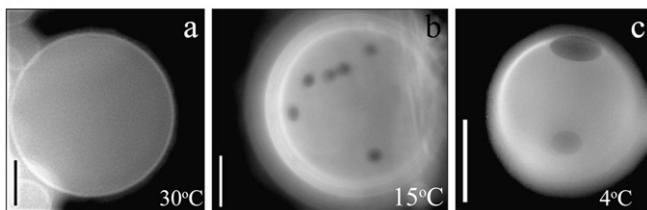**B 7-DEHYDROCHOLESTEROL**

Fig. 3. Domain morphology in ternary mixtures of EPC/ESM/sterol (34/33/33 mol%). (A) cholesterol and (B) 7-dehydrocholesterol. Domain separation was revealed using the fluorescent lipid Texas red-DPPE (1 mol%). Observation temperatures are reported as indicated. Bar = 20 μm. EPC, egg yolk L-α-phosphatidylcholine; ESM, egg yolk sphingomyelin.

The ability of sterols to form a L_o phase was conveniently denoted as promoter or inhibitor by Beattie et al. (35). The authors showed that vesicles containing ''promoter'' sterols (such as cholesterol, ergosterol, 25-hydroxycholesterol, epicholesterol, and dihydrocholesterol) separated into coexisting liquid phases as the temperature lowered through the miscibility transition temperature. In contrast, vesicles containing the "inhibitor" sterols (such as androstenolone, cholestenone, and cholestane) showed coexisting gel and liquid phases. On this simple basis, the assignment of 7-DHC to one of these two categories is problematic as we have observed that 7-DHC can form micrometer-scale domains but at a slower rate compared with cholesterol. Thus the small-sized domains formed by 7-DHC are characterized by a slower rate of fusion to create large domains, and their boundaries are more rigid than CHOL domains.

Synchrotron X-ray diffraction studies

The phase behavior of ESM/sterol mixtures was examined by X-ray diffraction in multilamellar dispersions as a function of sterol structure and concentration. The study focused on the association of the two most prominent membrane raft components, SM and sterol. An overview of the small-angle X-ray scattering (SAXS) recordings is presented in **Fig. 4A** during the heating temperature ramp from 20° to 50°C. The first two orders of Bragg reflections of the lamellar repeat are shown enlarged in the SAXS diffractogram. The splitting of the peaks reveals the heterogeneity of the mixture. Differences in the thermotropic behavior between mixtures containing either CHOL (Fig. 4A, left panel) or 7-DHC (Fig. 4A, right panel) are also evidenced by distinct lamellar repeat spacings. As expected, increased proportions of sterols in the mixtures result in a decrease in the lamellar repeat spacing (d-spacing) at low

temperatures (Fig. 4B). The "buffering" effect of cholesterol on the dimensions of the repeat unit as a function of temperature is explained by a compensatory disordering/ordering influence on the gel/disordered state, respectively. However, this influence is less marked for 7-DHC compared with CHOL as a function of temperature (Fig. 4B). For example, at 20°C the mixture containing 50 mol% CHOL forms a structure with two distinct coexisting structures (d-spacing 6.02 and 6.15 nm). Such heterogeneity is hardly detected in a mixture containing 50 mol% 7-DHC (6.27 and 6.30 nm). Because both the hydration layer thickness and the bilayer thickness contribute to the total d-repeat, their values have to be judged after Fourier deconvolution of the transversal electron profiles (**Fig. 6**). However, it is clear from the raw data that the two components in the diffractogram of the heterogeneous mixture show not only distinct d-spacing but also a different temperature variation in the presence of CHOL or 7-DHC (Fig. 4B).

In binary mixtures with a low proportion of sterol (10 mol%) [Fig. 4B(a)], there is no variation of d-spacing in the lowest temperature range. When the temperature is increased, the variation is biphasic: the d-spacing increases and then decreases with heating. We have interpreted the increase observed at a temperature lower than the onset of the gel-to-liquid transition as the transition of an interdigitated gel phase of sphingomyelin to a noninterdigitated arrangement that was already described for pure sphingomyelin (31). A visual inspection of the SAXS profiles at high temperatures reveals coexisting phases. However, applying the procedure of deconvolution to partially resolved peaks as shown in Fig. 5, the coexistence is detectable in the whole temperature range for sterol concentrations greater than 20 mol%.

Remarkably, in the presence of a sufficient concentration of CHOL, a structure detected throughout the temperature range shows a constant d-repeat [Fig. 4B(d)]. This temperature criterion has served previously to characterize the liquid-ordered phase identified by ESR in sphingomyelin/cholesterol mixtures at concentrations of sterol greater than 17 mol% (31). The stability of the structure suggests a fixed composition and temperature-independent behavior of the molecular arrangement of cholesterol with SM. Notably the heterogeneity is detected by SAXS in sterol-enriched mixtures around mammalian body temperatures (37°C) and upward when the d-spacings of the coexisting components diverge; the L_o component remains relatively unchanged while the d-spacing of the less-ordered component progressively decreases with increasing temperature (Fig. 4B).

To examine the localization of the sterol molecule within the coexisting structures and to measure the thickness of the hydration layer and the lipid bilayer in liposomes, electron density profiles perpendicular to the bilayer plane were calculated. Fourier syntheses were applied on the components separated after peak fitting of the raw diffractogram (Fig. 5) where peak 1 is assigned to the L_o structure characterized by a longer, relatively temperature-independent d-spacing, and peak 2 to the L_d
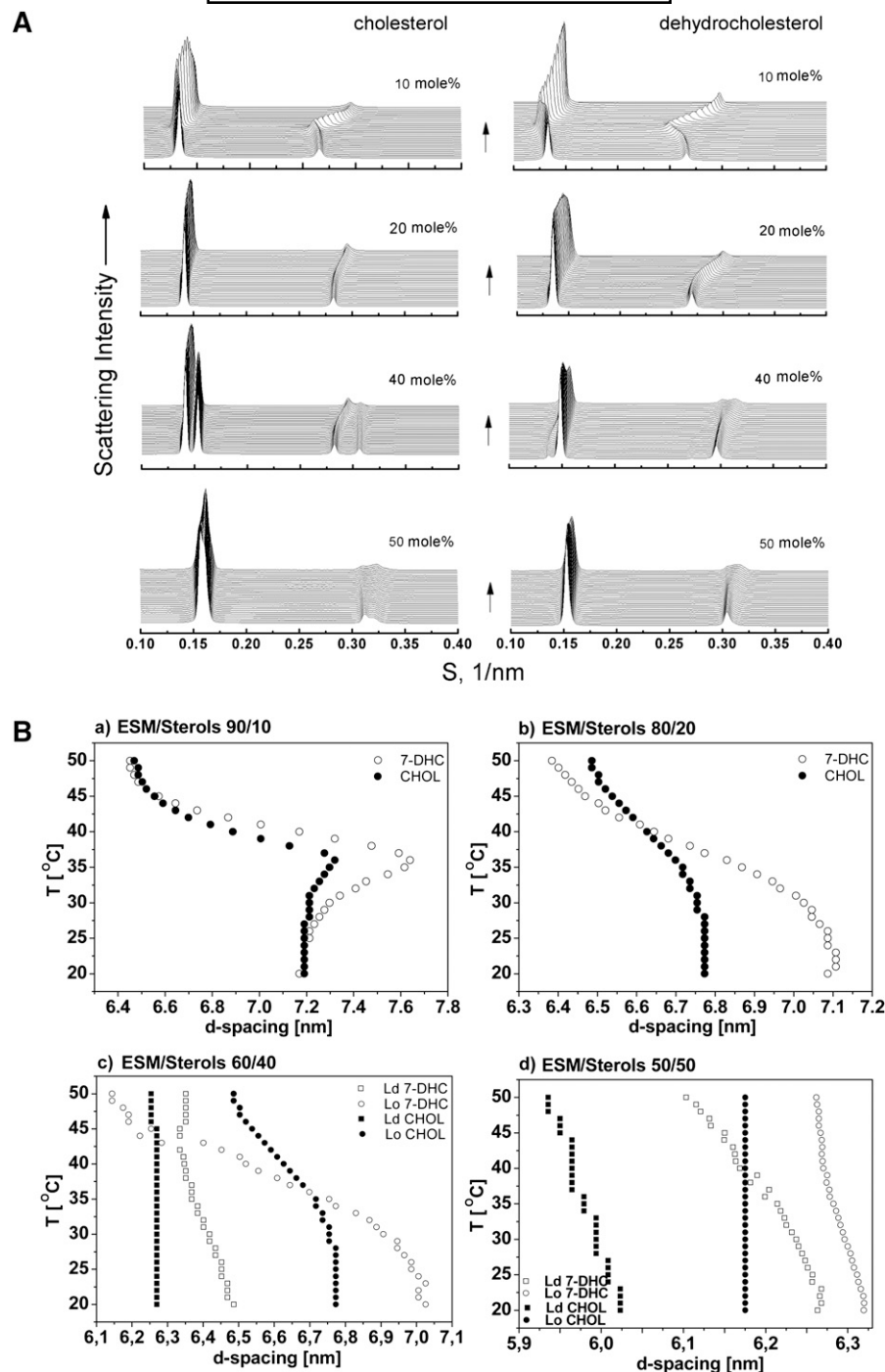
Fig. 4. SAXS showing the first and second order of the lamellar Bragg reflections of an aqueous liposomal dispersion of ESM/sterol mixtures (A). Lipid proportions are given as mol%. Samples were firstly equilibrated at 20°C and diffractograms were subsequently recorded at 1°C interval during heating to 50°C (rate +2°C/min shown by arrows). (B) Plots of the temperature dependence of the distinct components identified by peak fitting of diffractograms shown in 4A. Variations of the d-spacings are shown as a function of the temperature for binary lipid mixtures. Filled circles = cholesterol; open circles = 7-dehydrocholesterol. CHOL, cholesterol; 7-DHC, 7-dehydrocholesterol; ESM, egg yolk sphingomyelin; L_d, liquid-disordered phase; L_o, liquid-ordered phase; SAXS, small-angle X-ray scattering.

structure, which is less ordered, has a shorter d-spacing, and is strongly temperature-dependent. In Fig. 6 the electron density profiles calculated for the liquid-ordered component (peak 1) is shown on the left, and the disordered component (peak 2) on the right. The electron density profile of the liquid-ordered as well as the liquid-disordered component of sterol-containing mixtures shows a shoulder or plateau of electron density between the dense phosphorus and oxygen-rich head-group position and the trough in the bilayer center (36). Such a pronounced
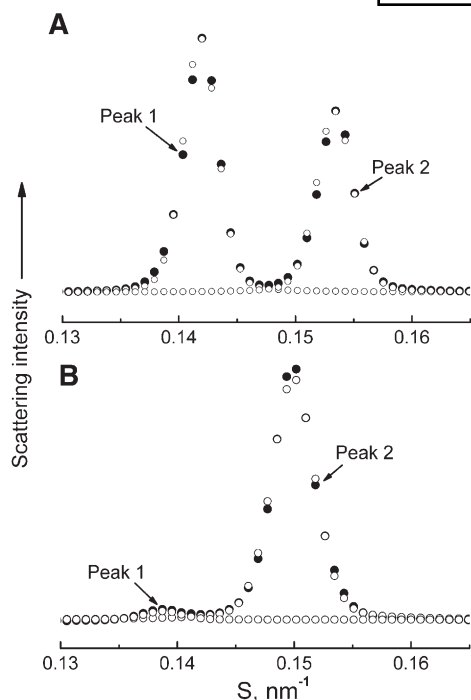
A

Fig. 5. Plots of first-order lamellar reflections (filled circles) recorded at 30°C for binary mixtures of (A) ESM codispersed with 40 mol% cholesterol and (B) 7-DHC. Peaks are fitted with Gaussian/Lorentzian curves (open circles) and separated into designated peak 1 (long d-spacing, liquid-ordered component) and peak 2 (liquid-disordered component). 7-DHC, 7-dehydrocholesterol; ESM, egg yolk sphingomyelin.

break in the slope of electron density is consistently detected in cholesterol-containing liposomes, which reflects the accurate alignment of the sterol nuclei at an accurate, precise depth in the bilayer. Electron density profiles for 7-DHC (dashed lines) have a smoother profile compared with cholesterol in both L_o and L_d structures. The difference is interpreted as 7-DHC occupying a position in the bilayer depth that is less constrained than cholesterol.

Phase coexistence in binary mixtures of SM with sterol is also evidenced by heterogeneous X-ray scattering in the wide-angle region, a measurement sensitive to the molecular ordering on a short distance compared with SAXS. The distinction between gel and fluid liquid-phase responses is shown in **Fig. 7A** for a control of pure SM (s = 1/d). The peak at d = 0.42 nm characterizing the gel phase disappears in the temperature interval coinciding with T_m of ESM (37°–41°C). In binary SM/sterol mixtures, the scattering signal in the wide-angle region can also be deconvolved by two components. The ordered phase is assigned to a d-spacing of 0.426 nm, which corresponds to the most "compact" phase, and the disordered phase (Fig. 7D, E) to a broad band centered at about 0.445 nm, which indicates longer average intermolecular distances. The position of both wide-angle bands remained constant with different proportions of sterol but their relative proportions in the heterogeneous scattering signal change. The change in the proportion of the two components of the wide-angle X-ray scattering

(WAXS) signal is illustrated in Fig.7. In the presence of 7-DHC, an abundant gel component is detected at 10 mol% in agreement with GUV and SAXS observations (Fig. 7D versus 7B in the presence of CHOL). More detail about the analysis of the WAXS intensity data is presented in the supplementary data.

ESR spectroscopic measurements

The motion and order in binary mixtures of ESM and sterols were investigated by ESR spectroscopy of a spin-labeled fatty acid with the nitroxide reporter group attached at position 16 of the acyl chain to probe the environment of the bilayer center. Order parameters and reorientation correlation times were derived from a spectral simulation analysis. The studies compared the properties of mixtures with different proportions of CHOL and 7-DHC.

ESM/sterol (83/17)

Order parameters and their assignments for these binary mixtures are presented in **Fig. 8A**. S_{zz} shows a marked decrease between 30° and 40°C, which likely corresponds to the $L_\beta \leftrightarrow L_d$ transition occurring in the same temperature range for pure ESM. The temperature dependence of S_{zz} has been analyzed as corresponding to a two-anisotropic sites system. It is observed that the values of the less-ordered B site below 30°C are aligned with the values of the more-ordered A site above 40°C, suggesting that they belong to the same L_o phase evidenced by the X-ray diffraction. Therefore L_β and L_o phases coexist below 30°C, and L_o and L_d (full line) coexist above 40°C. At 32°C and 37°C there is possibly coexistence of three phases L_β, L_o, and L_d, but their respective contribution cannot be reliably obtained. At 32°C the S_{zz} value assigned to L_o is underestimated, owing possibly to an unresolved contribution of the L_d phase. The disappearance of L_β above 37°C entails an enhancement of L_o and L_d fractions, which shows the same abundance at 42°C (Fig. 8B). Above this temperature, the L_o fraction decays with a corresponding increase of the L_d fraction.

ESM/sterol (66/34)

In the whole temperature range, the spectral fittings are consistent with the coexistence of L_o and L_d phases (Fig. 8C) in agreement with X-ray data. The L_o fraction reported by the doxyl-16-stearic acid is nearly independent of temperature with 0.83 ± 0.026 and 0.81 ± 0.031 for ESM mixtures with CHOL and 7- DHC, respectively (Fig. 8D). In the L_o phase, S_{zz} is similar for CHOL and 7-DHC, but in the L_d phase, S_{zz} is larger above 25°C for 7-DHC than for CHOL (Fig. 8C). This difference suggests that the fraction of sterols that is present in the L_d phase forms transient complexes with ESM (37) that are possibly distinct for the two sterols reported by ESR. For the stable assembly in L_o, the influence is similar for the two sterols.

ESM codispersed with 41, 50, and 60 mol% sterol

When the sterol concentration is increased to 40 mol% or greater, the assumption of an anisotropic site and an isotropic one yields better ESR spectral fittings than two anisotropic sites observed at 17 and 34 mol% (Fig. 8A–D).
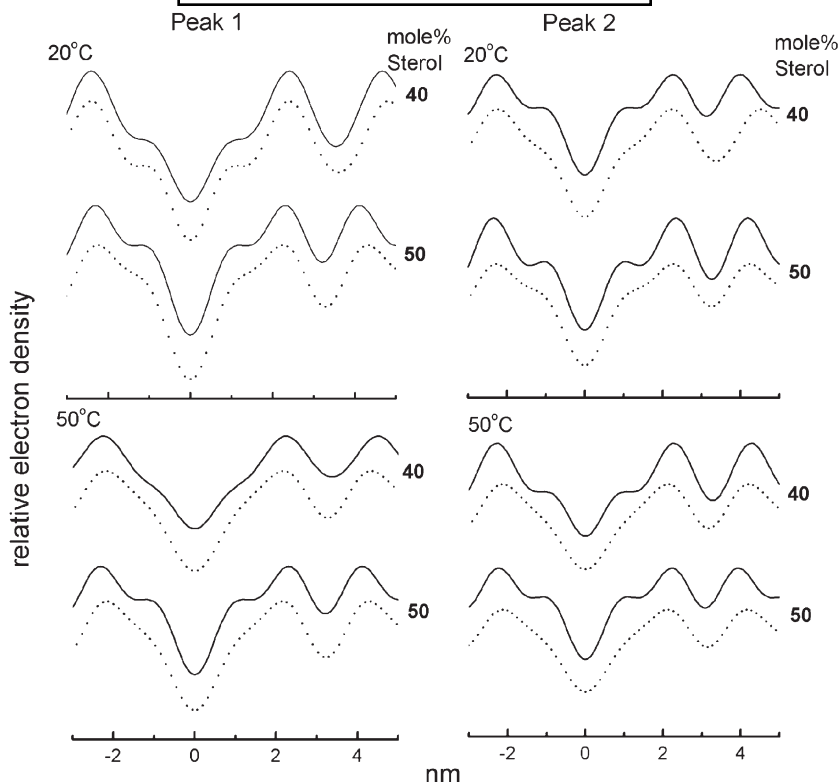
Fig. 6. Transversal electron density profiles of the two structures deconvolved from the aqueous dispersion of binary mixtures of ESM/cholesterol (solid line) and ESM/dehydrocholesterol (dashed line). Concentration are in mol% for recording at 20° and 50°C as indicated. Peaks 1 and 2, as indicated in Fig. 5, correspond to the lamellar liquid-ordered and liquid-disordered components separated from the raw diffractograms (Fig. 4A) by peak fitting (**Fig. 5**). ESM, egg yolk sphingomyelin.

At high concentration of sterol, the isotropic fraction remains constant at 0.04 ± 0.01 independently of temperature. The anisotropic site is assigned to the prominent L_o phase evidenced by X-ray diffraction at high concentration of sterol. The isotropic fraction likely corresponds to the probe located around the boundaries of domains of the L_o phase, undergoing exchange at a rate of $8 \times 10^6 - 10^7 \, s^{-1}$ with the probe incorporated in this phase. Fig. 8E–G shows only small differences between the S_{zz} values corresponding to ESM mixtures with CHOL or 7-DHC.

A comparison of spin-label motional parameters and activation energies derived from the spectroscopic measurements is presented in Table 1. Activation energies of the CHOL mixtures tended to be greater than mixtures containing 7-DHC, but no trend could be clearly discerned from the data on motional parameters.

DISCUSSION

Many biological studies have demonstrated that the structure of sterol has evolved to meet the specific requirements for the maintenance of biological membrane function. The maintenance of the liquid-crystalline structure in homeothermic mammalian species is especially challenging compared with poïkilotherms. The homeoviscous adaptation of unicellular organisms and plants to temperature is mainly controlled by the activity of desaturases responsible for inserting *cis*-double bonds into fatty acyl components of membrane lipids. Less attention has been given to sterol "acclimatization." In man, 19 enzymes are required after the cyclization of squalene, which leads to the final cholesterol nucleus. It is remarkable that the penultimate structure in the pathway, 7-dehydrocholesterol, with only a difference of an extra double bond in the B-ring of the sterol nucleus, does not meet the stringent requirements needed to substitute for cholesterol in deficited embryos with Smith-Lemli-Opitz syndrome.

Evidence that 7-DHC and cholesterol could not be interchanged had been obtained earlier for the restoration of the serotonin-binding capability of solubilized hippocampal receptor 1A in vitro (15, 16). Desmosterol, a closely related structure with an extra double bond ($\Delta24$) on the hydrocarbon side chain and also an immediate precursor of cholesterol in the Steinberg biosynthesis pathway, was also unable to substitute for cholesterol in the restoration of serotonin binding (38). Taken together, such biological studies have rarely received supporting evidence from detailed biophysical measurements to give credence to the concept proposed earlier by Bloch (39) that the "structural details of the cholesterol molecule and related sterols can be rationalized in terms of optimal hydrophobic interactions between the planar sterol ring system (and lateral side chain) and phospholipid acyl chains or ceramides" (21).

Following introduction of the so-called membrane raft hypothesis, which relies on the creation of sphingolipid/sterol
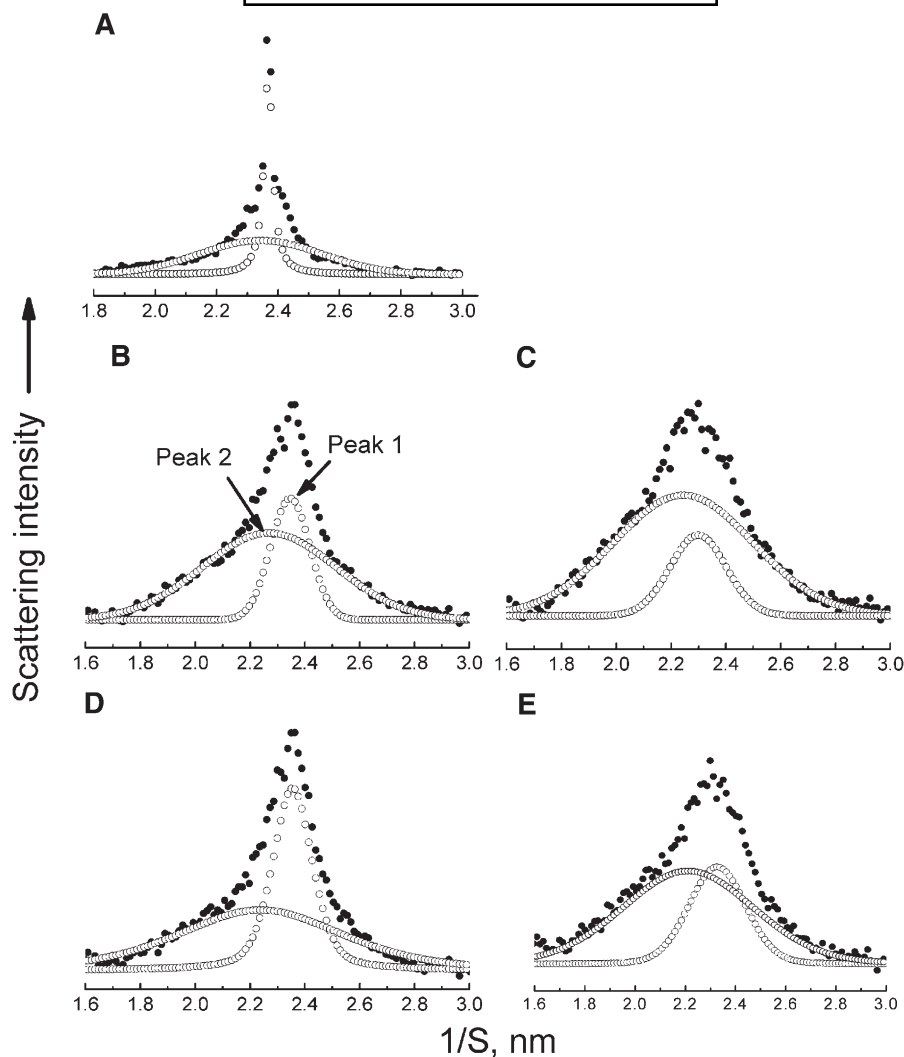
Fig. 7. Deconvolution of WAXS intensity profiles recorded at 30°C for the aqueous dispersion of (A) ESM (no sterol added). Binary mixtures ESM/cholesterol (B) 90/10 mol% and (C) 80/20 mol% are compared with ESM/7-DHC at (D) 90/10 mol% and (E) 80/20 mol%. 7-DHC, 7-dehydrocholesterol; ESM, egg yolk sphingomyelin; WAXS, wide-angle X-ray scattering.

enriched domains (40), a number of biophysical studies have emphasized the particular features of sterol structure in the separation of liquid-disordered from liquid-ordered domains (20, 41). The structural requirements have been operationally established from differential detergent solubilization of the L_o and L_d phases and by fluorescence quenching in stabilizing or disrupting lipid domains at different temperatures (42). The comparative studies have shown that the separation of a sterol-enriched domain formed with a saturated phospholipid, either SM or dipalmitoyl/phosphatidylcholine, can be counteracted by another sterol or steroid structure. This type of competition has possible consequences in SLO-affected fetus where the cholesterol of maternal origin and the endogenous 7-DHC are accumulating.

Binary and ternary lipid mixtures have been used for simple model membrane studies where the precision of biophysical methods can be fully exploited. This approach sacrifices the influence of minor lipid species of lipid on the L_o/L_d phase separation. This influence may not be insignificant as shown recently by examining the role of ceramide in quaternary mixtures in modulating the effect of sterol to counteract the separation of the L_β phase formed by the saturated sphingolipids at physiological temperatures (21, 43). Furthermore, in another X-ray diffraction study of ternary mixtures composed of egg phosphatidylcholine/sphingomyelin/cholesterol, several quasi at-equilibrium lipid organizations were said to exist at different times in the same local patch of membrane under conditions leading to L_o/L_d phase separation (44). The authors state that "identification of the conditions which can mimic heterogeneous dynamic membrane states in a lipid membrane model is a challenge. This is of particular importance as the lateral organization of lipid mixtures in fully equilibrated samples may differ from the arrangement found in quasi at-equilibrium conditions." These problems have been reviewed in the context of data obtained using a variety of biophysical techniques (45). In the present study, we have focused on a comparison of cholesterol with its precursor metabolite in simplified binary mixtures, which
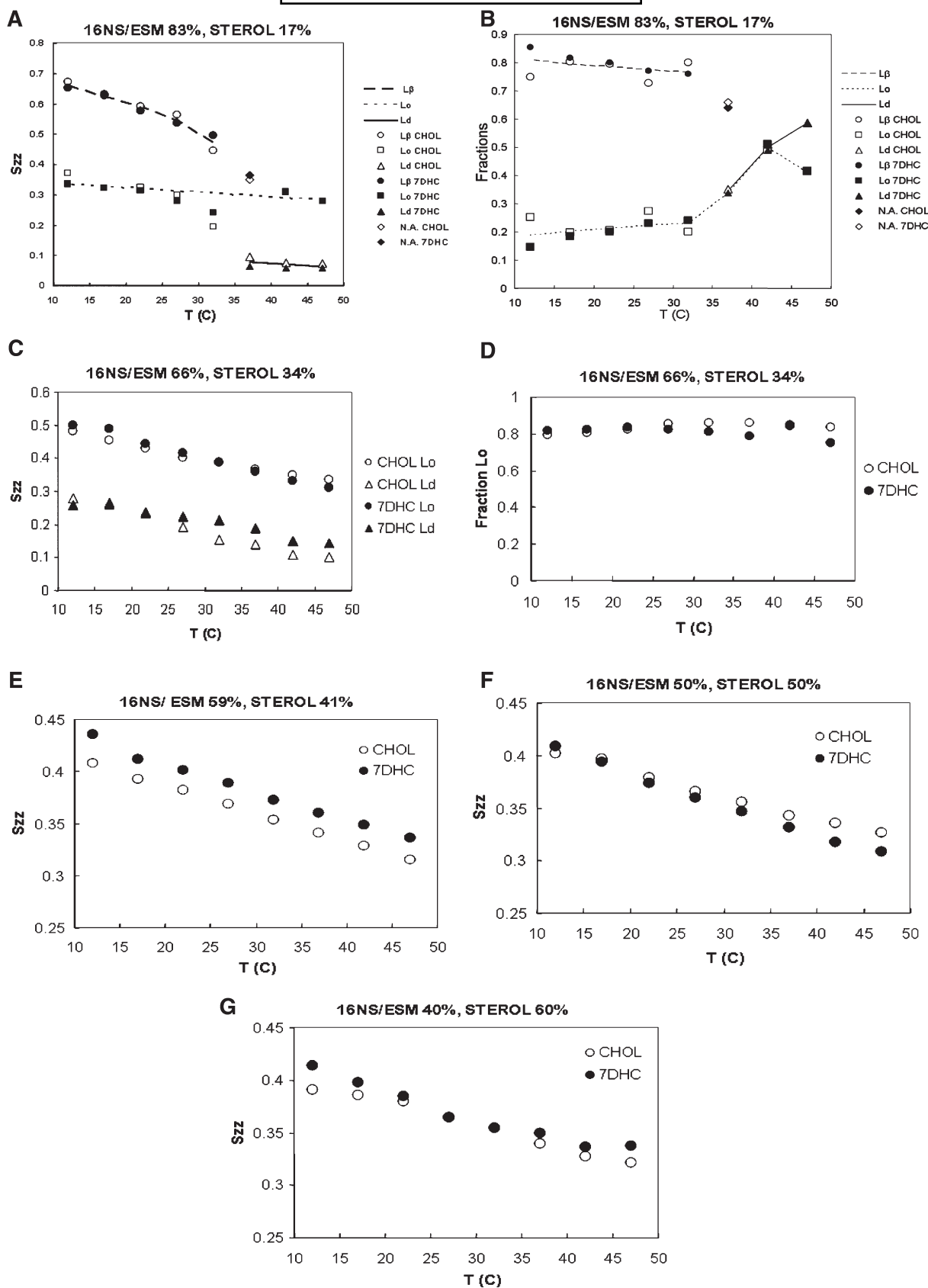
Fig. 8. Order parameters and fractions of the 16 NS spin-labeled probe in the distinct environments distinguished by spectral simulation in ESM/sterol binary mixtures. Proportions are given as mol%: phase assignments are based on ESR and X-ray observations (NA, no assignment). CHOL, cholesterol; 7-DHC, 7-dehydrocholesterol; EPC, egg yolk L-α-phosphatidylcholine; ESM, egg yolk sphingomyelin; L$_\beta$, gel phase; L$_d$, liquid-disordered phase; L$_o$, liquid-ordered phase; S$_{zz}$, order parameter; T(C), temperature °C.

can be readily related to earlier studies of sphingomyelin/cholesterol binary mixtures (27, 31).

The present study illustrates how subtle differences in the structure of the sterol nucleus may cause membrane lipid dysfunctions that "cascade" to create major consequences, such as SLO syndrome. The differences between cholesterol and 7-DHC can be summarized as follows: *1*) At the molecular level, the electron density profiles of the L_o and L_d phases suggest a slightly different arrangement of cholesterol and 7-DHC relative to the lipid/water interface of the host sphingomyelin bilayer. The overall geometry of the assembly with SM is not significantly altered in terms of the thickness of the bilayer and hydration layer, but an alteration in the electron density profile of bilayers is observed. Bilayers containing 7-DHC do not show a pronounced plateau assigned to the electron-enriched position of the sterol nucleus as they do in the case of cholesterol (28. 36). *2*) Because the sterol nucleus is rigid and localized superficially in the bilayer compared with the long hydrocarbon chains of SM, it is surprising that a slightly different positioning of the nucleus will have a consequence on the dynamics of spin-label motion in the center of the bilayer. However, ESR spectroscopy detects a subtle but significant alteration in the molecular order parameter of 16NS in both of the coexisting phases of the heterogeneous binary mixture. In the bilayer center, the ordering influence of cholesterol is weak relative to positions closer to the lipid-water interface where the flat and rigid sterol ring system is intercalated. Nevertheless, an increase in S_{zz} for 16NS from 0.11 (pure L_d at 41°C) to 0.30 was already detected in the L_o phase applying similar ESR and spectral simulation methods (31). The present ESR observations show a stronger influence of 7-DHC in the bilayer center compared with cholesterol. We assume that the anchoring of the cholesterol nucleus at a more precise depth of the bilayer would limit its influence on regions around the bilayer center. Looser van der Waals interactions of the 7-DHC ring with the hydrocarbon chains of sphingomyelin can be expected to cause the averaging of the position of 7-DHC along the bilayer normal. It is also possible that the stabilization by 3-hydroxyl group of cholesterol, which participates in a precisely configured hydrogen-bond network formed with amino groups of the sphingosine moiety, is not permitted in the case of a loosely associated sterol such as 7-DHC. *3*) Sterol-sphingomyelin interaction prevents the separation of the gel phase composed of the sphingomyelin molecular species at temperatures lower than their respective transitions. As observed from the WAXS measurements, the complete replacement of the gel phase is not seen until the proportion of either of the two sterols reaches 34 mol%. WAXS analysis indicates a greater abundance of a gel component in the presence of 7-DHC than cholesterol at 10 and 20 mol%. ESR methods cannot detect the difference evidenced by WAXS, and the binary mixture at 17 mol% 7-DHC and cholesterol is composed of equally abundant gel/fluid fractions. Note that the partition of the 16NS spin label may obscure the actual abundance of the fractions. At higher temperatures and sterol concentration, the heterogeneity of WAXS signal can be traced by peak deconvolution, demonstrating the coexistence of a compact ordered phase with loosely oriented acyl chains. *4*) A remarkable result is that differences between sterols detected by WAXS and ESR in the nanometer range are translated into differences on the long distance scale documented by SAXS and GUV observations. The difference between 7-DHC– and cholesterol-containing liposomes detected by SAXS for intermediate sterol concentrations illustrates this point. While cholesterol at 40 mol% produces a clear-cut separation revealed by distinct Bragg's reflections of the SAXS, 7-DHC produces only a shoulder of the diffraction peak. The difference between the two sterols is widened by changing the temperature. Taking into account the GUV observations showing the small-sized domains formed in the presence of 7-DHC, we assume that the cause of irregular arrays is a loose alignment of the small-sized domains formed in the adjacent liposome layers. The rigidity of domains created in mixtures containing 7-DHC can explain the different diffraction pattern compared with cholesterol. Nevertheless, the methods of SAXS peak fitting and calculation of the transversal electron density profile have been able to detect differences between sterols while the geometry of the SM/sterol assembly is almost the same. *5*) Because it is can be inferred from WAXS and ESR that cholesterol and 7-DHC do not intercalate similarly to disrupt the gel phase composed of pure sphingomyelin, it is expected that imaging of domains at a low temperature (22°C) provided by the GUV observations will be different. Indeed, the domains of 7-DHC/sphingomyelin separated from the fluid, brightly fluorescent host phospholipid appear with crenulated boundaries and a small size. Their aspect and temperature behavior are more reminiscent of gel-like domains than they are of the large, round-shaped, rapidly merging domains that are observed in the presence of cholesterol and are typical of a liquid phase. The present data are in agreement with Langmuir monolayers data showing that the molecular area in 7-DHC/dipalmitoylphosphatidylcholine film is larger than for mixtures containing cholesterol (46). Another monolayer study has reported no significant difference between 7-DHC and cholesterol in mixtures with EPC (47). Therefore the monolayer studies with 7-DHC have concluded that the difference with cholesterol is likely found in the L_o domains formed with the saturated lipids. This result is fully consistent with the present GUV and X-ray examination and is partially consistent with present ESR data showing differences in the less-ordered coexisting phase.

Besides the composition and biophysical properties of the raft membranes, the size of domains has also emerged as a factor influencing the efficiency of the multiprotein signaling machinery (48). It was found that enrichment in 7-dehydrocholesterol causes raft instability as judged by detergent solubilization and methyl-cyclodextrin extractability. As a consequence, it was pointed out in the same study that the raft-altered structure resulted in a hyperallergic response of mast cells prepared from Dhcr7$^{-/-}$ mice (19). More specifically, mast cells derived from 7-DHC reductase knockout mice show a high cytokine production

with a potentiated degranulation reaction after stimulation of IgE receptors. This result was tentatively explained as a disruption of lipid rafts such that *Lyn* kinase was displaced from the raft leading to loss of regulatory activity exerted by *Lyn* on *Fyn* kinase activity, Akt phosphorylation, and degranulation. Indeed, the demonstration of the raft proteome alterations in the study is based on the recovery of detergent resistant membranes (Triton at 0.075%–0.1%, 30°C), an operation criticized because of possible artifacts of protein redistribution [for instance, Prion and some Thy-1 are redistributed between membranes comprised of DRM prepared from neuronal cell membranes (49)].

Because of inherent problems with detergent treatment in isolating membrane rafts, greater emphasis has been placed on model membrane studies. Precautions are warranted in biophysical investigations of such simple systems prepared in vitro. Nevertheless other difficulties are becoming apparent. For example, the peak-width parameter to measure domain size using the Sherrer equation applied to Bragg reflections is not reliable in the liquid crystalline state. Spectroscopic methods may also require highly reproducible conditions of temperature, time of equilibration, and pretreatment that affect sample presentation before measurement. It is known that the curvature of liposome lamellae influences the derived parameters and may yield information of doubtful physiological relevance. Because of these limitations, we have used three different methods in our assessment of the domain size in the comparison of cholesterol and its precursor. This combination of approaches improves reliability of conclusions regarding an understanding of how a minor alteration of the sterol ring structure affects the molecular assembly from the molecular to the micrometer scale.

It is striking that the treatment recommended by pediatricians for affected children combines cholesterol supplementation and administration of simvastatin to inhibit HMG-CoA reductase and, hence, aberrant sterol synthesis (50). The results were judged positive or conjectural (51, 52). The difference in the structure of sterols can play a role in membrane organization and the sorting of the morphogenic protein Sonic Hedgehog, but it can also expose membranes to hazards associated with free-radical oxidations (53). It is known that 7-DHC is sensitive to oxygen and ultraviolet light. An assessment of the benefit provided by the treatment on membrane structure and stability is now under investigation using erythrocytes from affected children. The results from this study and biophysical data will guide understanding of the teratology of Smith-Lemli-Opitz syndrome.[jlr]

REFERENCES

1. Smith, D. W., L. Lemli, and J. M. Opitz. 1964. Newly recognised syndrome of multiple congenital anomalies. *J. Pediatr.* **64:** 210–217.
2. Tint, G. S., H. W. Yu, Q. Shang, G. R. Xu, and S. B. Patel. 2006. The use of the Dhcr7 knockout mouse to accurately determine the origin of fetal sterols. *J. Lipid Res.* **47:** 1535–1541.
3. Waterham, H. R. 2006. Defects of cholesterol biosynthesis. *FEBS Lett.* **580:** 5442–5449.
4. Witsch-Baumgartner, M. 2008. DHCR7 mutations causing the Smith-Lemli-Opitz syndrome. *Future Lipidol.* **3:** 585–593.
5. Chevy, F., L. Humbert, and C. Wolf. 2005. Sterol profiling of amniotic fluid: a routine method for the detection of distal cholesterol synthesis deficit. *Prenat. Diagn.* **25:** 1000–1006.
6. Jira, P. E., H. R. Waterham, R. J. A. Wanders, J. A. M. Smeitink, R. C. A. Sengers, and R. A. Wevers. 2003. Smith-Lemli-Opitz syndrome and the DHCR7 gene. *Ann. Hum. Genet.* **67:** 269–280.
7. Porter, F. D. 2003. Human malformation syndromes due to inborn errors of cholesterol synthesis. *Curr. Opin. Pediatr.* **15:** 607–613.
8. Porter, F. D. 2006. Cholesterol precursors and facial clefting. *J. Clin. Invest.* **116:** 2322–2325.
9. Chevy, F., F. Illien, C. Wolf, and C. Roux. 2002. Limb malformations of rat fetuses exposed to a distal inhibitor of cholesterol biosynthesis. *J. Lipid Res.* **43:** 1192–1200.
10. Barbu, V., C. Roux, D. Lambert, R. Dupuis, J. Gardette, J-C. Maziere, C. Maziere, E. Elefant, and J. Polonovski. 1988. Cholesterol prevents the teratogenic action of AY 9944: importance of the timing of cholesterol supplementation to rats. *J. Nutr.* **118:** 774–779.
11. Fitzky, B. U., F. F. Moebius, H. Asaoka, H. Waage-Baudet, L. W. Xu, G. R. Xu, N. Maeda, K. Kluckman, S. Hiller, H. W. Yu, et al. 2001. 7-Dehydrocholesterol-dependent proteolysis of HMG-CoA reductase suppresses sterol biosynthesis in a mouse model of Smith-Lemli-Opitz/RSH syndrome. *J. Clin. Invest.* **108:** 905–915.
12. Honda, M., G. S. Tint, A. Honda, L. B. Nguyen, T. S. Chen, and S. Shefer. 1998. 7-dehydrocholesterol down-regulates cholesterol biosynthesis in cultured Smith-Lemli-Opitz syndrome skin fibroblasts. *J. Lipid Res.* **39:** 647–657.
13. Ehtesham, M., A. Sarangi, J. G. Valadez, S. Chanthaphaychith, M. W. Becher, T. W. Abel, R. C. Thompson, and M. K. Cooper. 2007. Ligand-dependent activation of the hedgehog pathway in glioma progenitor cells. *Oncogene.* **26:** 5752–5761.
14. Korade, Z., and A. K. Kenworthy. 2008. Lipid rafts, cholesterol, and the brain. *Neuropharmacology.* **55:** 1265–1273.
15. Chattopadhyay, A., Y. D. Paila, M. Jotfurulla, A. Chaudhuri, P. Singh, M. Murty, and M. Vairamani. 2007. Differential effects of cholesterol and 7-dehydrocholesterol on ligand binding of solubilized hippocampal serotonin(1A) receptors: implications in SLOS. *Biochem. Biophys. Res. Commun.* **363:** 800–805.
16. Singh, P., Y. D. Paila, and A. Chattopadhyay. 2007. Differential effects of cholesterol and 7-dehydrocholesterol on the ligand binding activity of the hippocampal serotonin(1A) receptor: implications in SLOS. *Biochem. Biophys. Res. Commun.* **358:** 495–499.
17. Keller, R. K., T. P. Arnold, and S. J. Fliesler. 2004. Formation of 7-dehydrocholesterol-containing membrane rafts in vitro and in vivo, with relevance to the Smith-Lemli-Opitz syndrome. *J. Lipid Res.* **45:** 347–355.
18. Kovarova, M., C. A. Wassif, S. Odom, K. Liao, F. D. Porter, and J. Rivera. 2006. Cholesterol deficiency in a mouse model of Smith-Lemli-Opitz syndrome reveals increased mast cell responsiveness. *J. Exp. Med.* **203:** 1161–1171.
19. Ollila, S. O. H., T. Rog, M. Karttunen, and I. Vattulainen. 2007. Role of sterol type on lateral pressure profiles of lipid membranes affecting membrane protein functionality: comparison between cholesterol, desmosterol, 7-dehydrocholesterol and ketosterol. *J. Struct. Biol.* **159:** 311–323.
20. Xu, X., R. Bittman, G. Duportail, D. Heissler, C. Vilcheze, and E. London. 2001. Effect of the structure of natural sterols and sphingolipids on the formation of ordered sphingolipid/sterol domains (rafts). *J. Biol. Chem.* **276:** 33540–33546.
21. Megha, B. O., and E. London. 2006. Cholesterol precursors stabilize ordinary and ceramide-rich ordered lipid domains (lipid rafts) to different degrees: implications for the Bloch hypothesis and sterol biosynthesis disorders. *J. Biol. Chem.* **281:** 21903–21913.
22. Gandhavadi, M., D. Allende, A. Vidal, S. A. Simon, and T. J. McIntosh. 2002. Structure, composition, and peptide binding properties of detergent soluble bilayers and detergent resistant rafts. *Biophys. J.* **82:** 1469–1482.
23. Angelova, M. I., and D. S. Dimitrov. 1986. Liposome electroformation. *Faraday Discuss.* **81:** 303–311.
24. Staneva, G., M. Seigneuret, K. Koumanov, G. Trugnan, and M. I. Angelova. 2005. Detergents induce raft-like domains budding and fission from giant unilamellar heterogeneous vesicles: a direct microscopy observation. *Chem. Phys. Lipids.* **136:** 55–66.

25. Veatch, S. L., I. V. Polozov, K. Gawrisch, and S. L. Keller. 2004. Liquid domains in vesicles investigated by NMR and fluorescence microscopy. *Biophys. J.* **86:** 2910–2922.

26. Maulik, P. R., and G. G. Shipley. 1996. N-palmitoyl sphingomyelin bilayers: structure and interactions with cholesterol and dipalmitoylphosphatidylcholine. *Biochemistry.* **35:** 8025–8034.

27. Quinn, P. J., and C. Wolf. 2009. Thermotropic and structural evaluation of the interaction of natural sphingomyelins with cholesterol. *Biochim. Biophys. Acta.* **1788:** 1877–1889.

28. McIntosh, T. J. 1978. Effect of cholesterol on structure of phosphatidylcholine bilayers. *Biochim. Biophys. Acta.* **513:** 43–58.

29. Quinn, P. J., and C. Wolf. 2009. Hydrocarbon chains dominate coupling and phase coexistence in bilayers of natural phosphatidylcholines and sphingomyelins. *Biochim. Biophys. Acta.* **1788:** 1126–1137.

30. Chachaty, C., and C. Wolf. 1999. An application of ESR spectral simulation methods to doxylstearic spin probes in pure and mixed sphingomyelin bilayers. Effect of sterol additives. *Mol. Phys. Reports.* **26:** 143–150.

31. Chachaty, C., D. Rainteau, C. Tessier, P. J. Quinn, and C. Wolf. 2005. Building up of the liquid-ordered phase formed by sphingomyelin and cholesterol. *Biophys. J.* **88:** 4032–4044.

32. Dietrich, C., L. A. Bagatolli, Z. N. Volovyk, N. L. Thompson, M. Levi, K. Jacobson, and E. Gratton. 2001. Lipid rafts reconstituted in model membranes. *Biophys. J.* **80:** 1417–1428.

33. Baumgart, T., S. T. Hess, and W. W. Webb. 2003. Imaging coexisting fluid domains in biomembrane models coupling curvature and line tension. *Nature.* **425:** 821–824.

34. Garcia-Saez, A. J., S. Chiantia, and P. Schwille. 2007. Effect of line tension on the lateral organization of lipid membranes. *J. Biol. Chem.* **282:** 33537–33544.

35. Beattie, M. E., S. L. Veatch, B. L. Stottrup, and S. L. Keller. 2005. Sterol structure determines miscibility versus melting transitions in lipid vesicles. *Biophys. J.* **89:** 1760–1768.

36. McIntosh, T. J., S. A. Simon, D. Needham, and C. H. Huang. 1992. Structure and cohesive properties of sphingomyelin cholesterol bilayers. *Biochemistry.* **31:** 2012–2020.

37. Radhakrishnan, A., and H. M. McConnell. 2007. Composition fluctuations, chemical exchange and nuclear relaxation in membranes containing cholesterol. *J. Chem. Phys.* **126:** 185101–185107.

38. Singh, P., R. Saxena, and Y. D. Paila. M. Jafurulla, and A. Chattopadhyay. 2009. Differential effects of cholesterol and desmosterol on the ligand binding function of the hippocampal serotonin1A receptor: implications in desmosterolosis. *Biochim. Biophys. Acta.* **1788:** 2169–73..

39. Bloch, K. E. 1979. Speculations on the evolution of sterol structure and function. *CRC Crit. Rev. Biochem.* **7:** 1–5.

40. Simons, K., and E. Ikonen. 1997. Functional rafts in cell membranes. *Nature.* **387:** 569–572.

41. Holopainen, J. M., A. J. Metso, J-P. Mattila, A. Jutila, and P. K. J. Kinnunen. 2004. Evidence for the lack of a specific interaction between cholesterol and sphingomyelin. *Biophys. J.* **86:** 1510–1520.

42. Wenz, J. J., and F. J. Barrantes. 2003. Steroid structural requirements for stabilizing or disrupting lipid domains. *Biochemistry.* **42:** 14267–14276.

43. Staneva, G., C. Chachaty, C. Wolf, K. Koumanov, and P. J. Quinn. 2008. The role of sphingomyelin in regulating phase coexistence in complex lipid model membranes: competition between ceramide and cholesterol. *Biochim. Biophys. Acta.* **1778:** 2727–2739.

44. Tessier, C., G. Staneva, G. Trugnan, C. Wolf, and P. Nuss. 2009. Liquid-liquid immiscibility under non-equilibrium conditions in a model membrane: an X-ray synhrotron study. *Colloids Surf. B Biointerfaces.* **74:** 293–297.

45. Quinn, P. J., and C. Wolf. 2009. The liquid-ordered phase in membranes. *Biochim. Biophys. Acta.* **1788:** 33–46.

46. Berring, E. E., K. Borrenpohl, S. J. Fliesler, and A. B. Serfis. 2005. A comparison of the behaviour of cholesterol and selected derivatives in mixed sterol-phospholipid Langmuir monolayers: a fluorescence microscopy study. *Chem. Phys. Lipids.* **136:** 1–12.

47. Serfis, A. B., S. Brancato, and S. J. Fliesler. 2001. Comparative behaviour of sterols in phosphatidylcholine-sterol monolayer films. *Biochim. Biophys. Acta.* **1511:** 341–348.

48. Pike, L. J. 2009. The challenge of lipid rafts. *J. Lipid Res.* **50(suppl):** S323–S328. doi:3

49. Chen, X., A. Jen, A. Warley, M. J. Lawrence, P. J. Quinn, and R. J. Morris. 2009. Isolation at physiological temperature of detergent-resistant membranes with properties expected of lipid rafts: the influence of buffer composition. *Biochem. J.* **417:** 525–533.

50. Chan, Y. M., L. S. Merkens, W. E. Connor, J. B. Roullet, J. A. Penfield, J. M. Jordan, R. D. Steiner, and P. J. Quinn. 2009. Effects of dietary cholesterol and simvastatin on cholesterol synthesis in Smith-Lemli-Opitz syndrome. *Pediatr. Res.* **65:** 681–685.

51. Jira, P. E., R. A. Wevers, J. de Jong, E. Rubio-Gozalbo, F. S. Janssen-Zijlstra, A. F. van Heyst, R. C. Sengers, and J. A. Smeitink. 2000. Simvastatin. A new therapeutic approach for Smith-Lemli-Opitz syndrome. *J. Lipid Res.* **41:** 1339–1346.

52. Haas, D., S. F. Garbade, C. Vohwinkel, N. Muschol, F. K. Trefz, J. M. Penzien, J. Zschocke, G. F. Hoffmann, and P. Burgard. 2007. Effects of cholesterol and simvastatin treatment in patients with Smith-Lemli-Opitz syndrome (SLOS). *J. Inherit. Metab. Dis.* **30:** 375–387.

53. Galea, A. M., and A. J. Brown. 2009. Special relationship between sterols and oxygen: were sterols an adaptation to aerobic life? *Free Radic. Biol. Med.* **47:** 880–889.